

Performance and calibration for the identification of boosted Higgs bosons decaying into beauty quark pairs in ATLAS

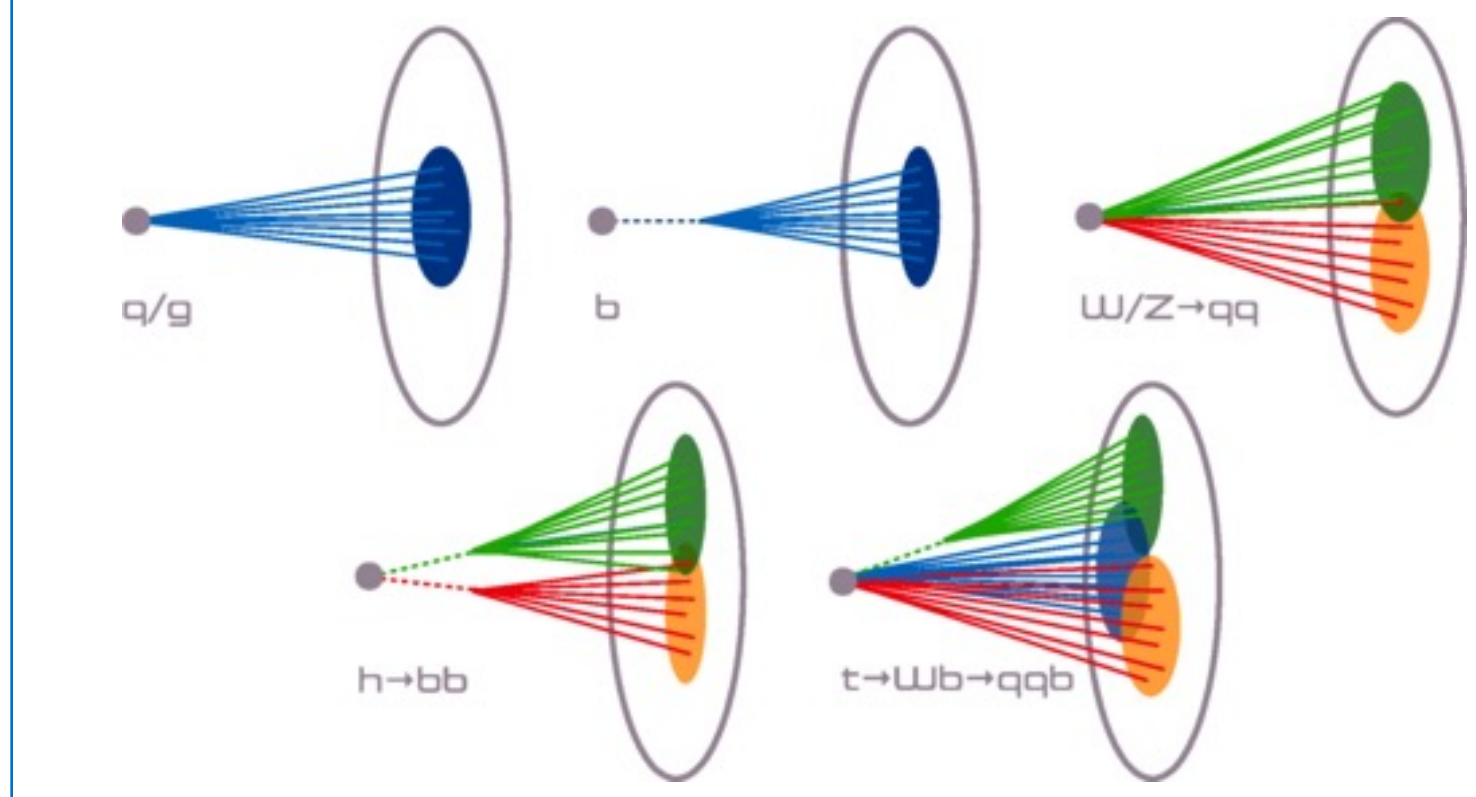


Figure 1: Pictorial representation of ordinary quark and gluon jets (top left), b jets (top centre), and boosted-jet topologies, emerging from high- p_T W and Z bosons (top right), Higgs bosons (bottom left), and top quarks (bottom right) decaying to all-quark final states [1].

Motivation

The decay of the Standard Model (SM) Higgs boson to a pair of beauty quarks, $H \rightarrow b\bar{b}$, has a branching fraction of 58%, the largest of the Higgs decay modes. There are many Beyond Standard Model (BSM) scenarios in which a high-transverse momentum (high- p_T) Higgs boson is produced in the decay of new heavy particles and BSM contributions can also impact the Higgs production differential cross-section, particularly at high- p_T . As the p_T of the Higgs boson increases, the $H \rightarrow b\bar{b}$ decay products become highly collimated and are contained within a large-radius (large- R) jet. Figure 1 shows the various jet topologies that are seen in ATLAS. Dedicated reconstruction techniques are critical to improving the sensitivity of searches for New Physics and for precise Standard Model measurements in this regime.

b -tagging in ATLAS

Variable radius (VR) track-jets containing single b -hadrons are identified using ‘low-level’ algorithms that are designed to exploit the specific features of b -hadron decays. The outputs of these taggers are combined into ‘high-level’ algorithms. There are currently two taggers used in ATLAS analyses: a boosted decision tree, MV2, or a deep neural network, DL1r, which is the latest tagger.

Performance

The three outputs from the $X \rightarrow b\bar{b}$ algorithm are combined into a single discriminant defined as:

$$D_{Xbb} = \ln \frac{p_{Higgs}}{f_{top} \cdot p_{top} + (1 - f_{top}) \cdot p_{multijet}},$$

where f_{top} determines the fraction of top background and is set to 0.25.

The distribution of this discriminant for the signal (Higgs-matched jets) and backgrounds (top-matched jets and multijet) is shown in Figure 2. The performance of the tagger is evaluated using the Higgs efficiency, ϵ , defined as the number of tagged jets divided by the total number of $H \rightarrow b\bar{b}$ jets, and the background rejection, $1/\epsilon$. The background rejections as a function of the Higgs efficiency are shown in Figure 3 for the multijet (left) and top (right), respectively. Jets are considered tagged if the value of D_{Xbb} is above a certain threshold; the 60% operating point is calibrated here.

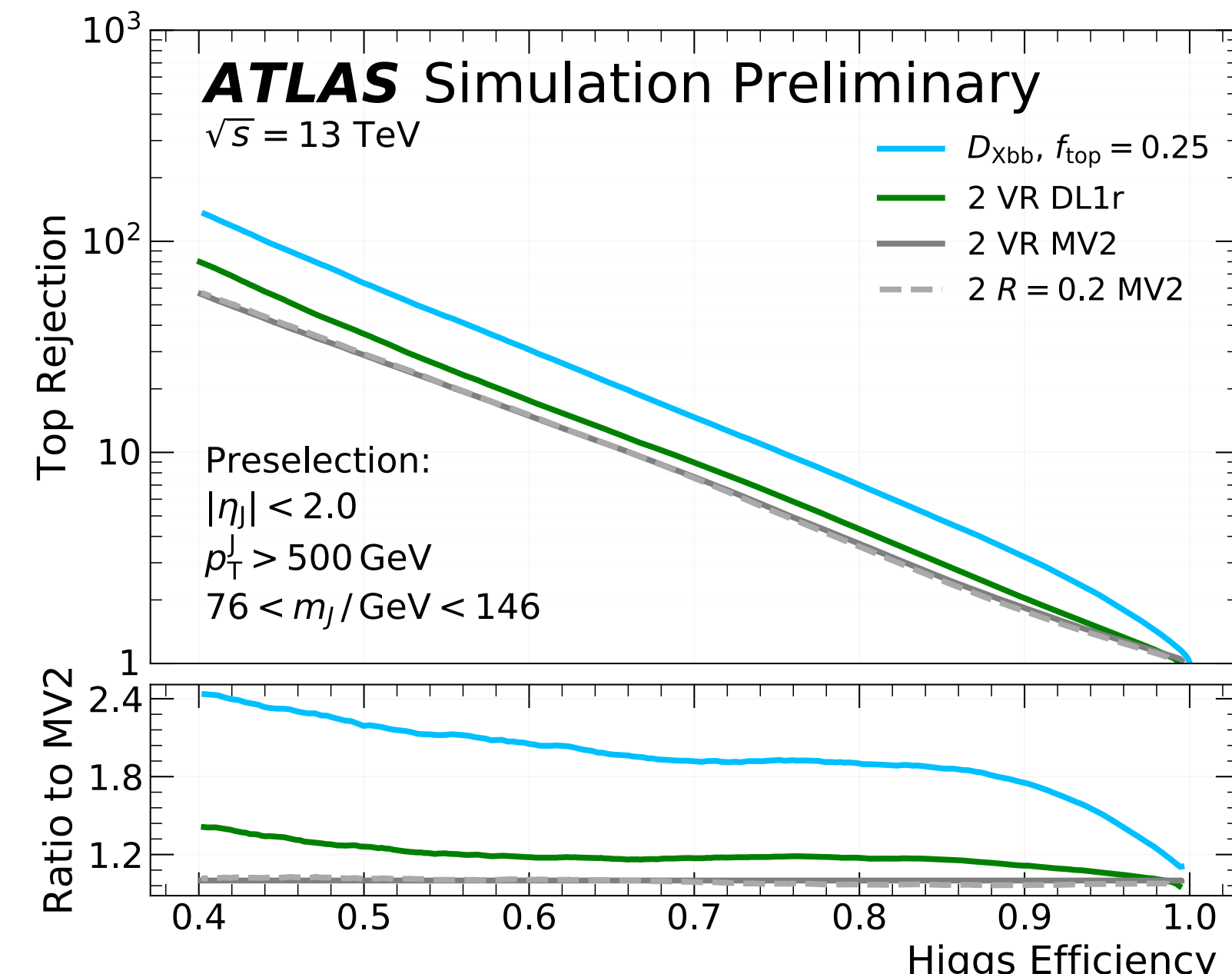
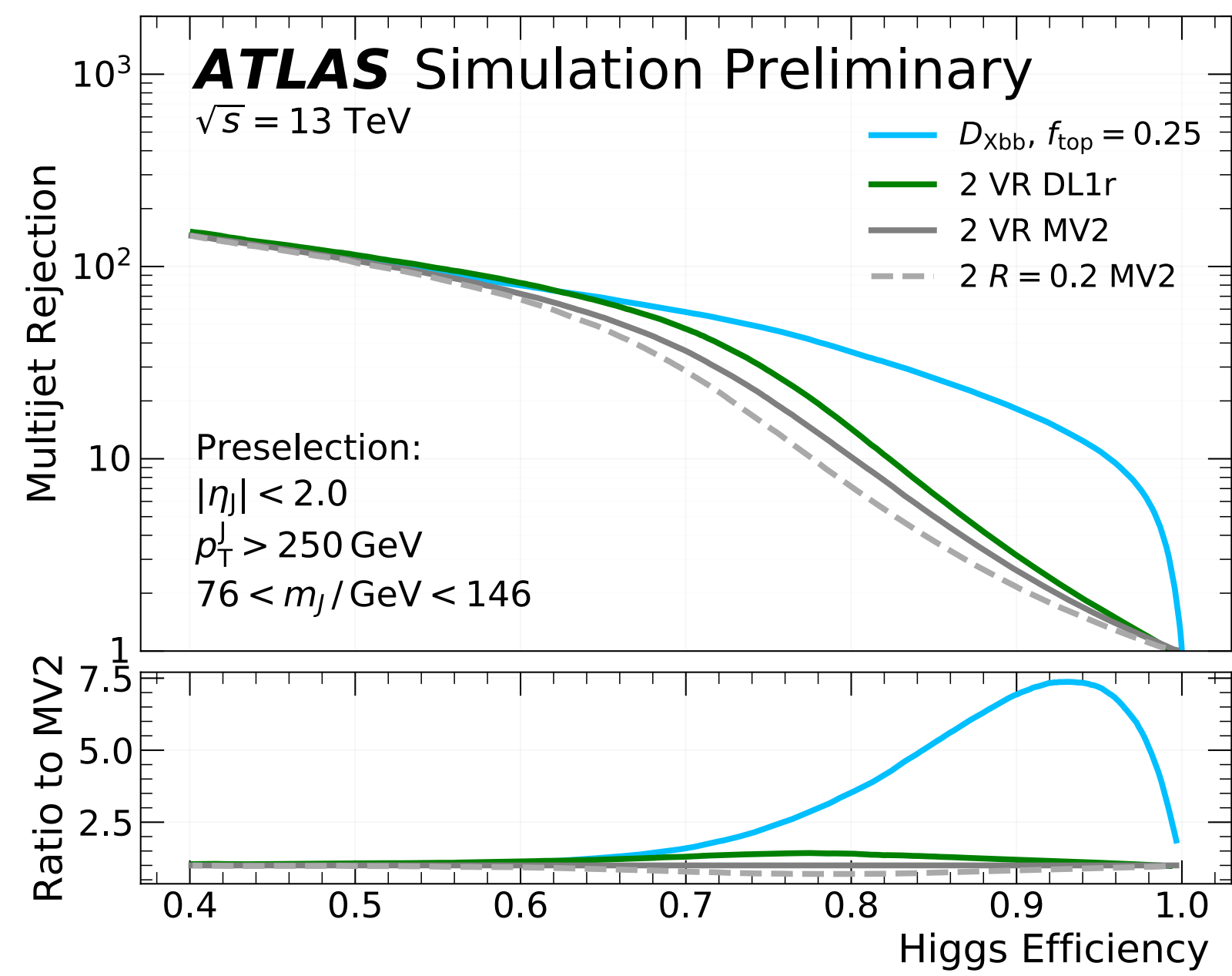


Figure 3: The multijet (left) and top (right) background rejection as a function of the Higgs efficiency for large- R jet $p_T > 500$ GeV for the $X \rightarrow b\bar{b}$ (blue). The performance of the DL1r (green) and two variants of the MV2 (grey) taggers are also shown for comparison [2].

The $X \rightarrow b\bar{b}$ tagger

The $X \rightarrow b\bar{b}$ tagger [2] is a new algorithm that aims to identify boosted $H \rightarrow b\bar{b}$ decays by tagging the large- R jet, which contains up to three VR track-jets. It is a feed-forward neural network that combines DL1r flavour tagging information of the track-jets, with the p_T and η of the large- R jet. The neural network provides three outputs corresponding to the probabilities for Higgs (p_{Higgs}), multijet ($p_{multijet}$) and top (p_{top}) process hypotheses.

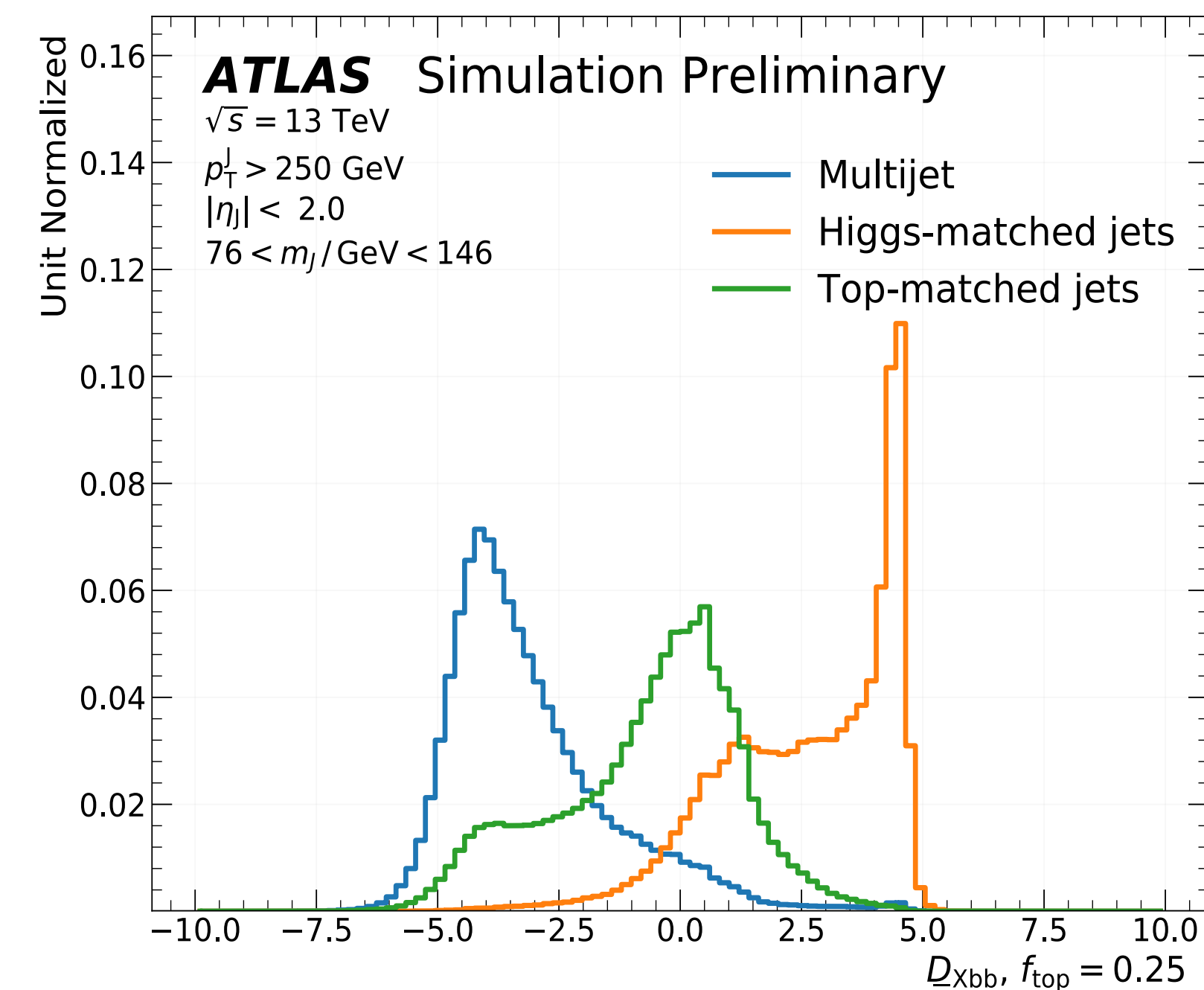


Figure 2: The discriminant distribution for the $X \rightarrow b\bar{b}$ algorithm, normalised to unity [2].

Signal efficiency calibration using $Z(\rightarrow b\bar{b}) + \text{jets}$ and $Z(\rightarrow b\bar{b})\gamma$ events

The efficiency measured in data can differ from that measured in simulation so a data-to-simulation scale factor is calculated in order to match the efficiencies:

$$SF = \frac{\epsilon_{data}}{\epsilon_{MC}} = \frac{\frac{N_{passed}^{data}}{N_{total}^{data}}}{\frac{N_{passed}^{MC}}{N_{total}^{MC}}} = \frac{\mu_{post-tag}}{\mu_{pre-tag}}.$$

$\mu_{pre-tag}$ and $\mu_{post-tag}$ are the signal strengths relative to the Standard Model expectation before and after tagging, respectively. To measure $\mu_{post-tag}$ in the $Z(\rightarrow b\bar{b})\gamma$ measurement, a binned likelihood template fit to the $b\bar{b}$ invariant mass spectrum is performed in the region $200 < p_T < 450$ GeV. For the $Z(\rightarrow b\bar{b}) + \text{jets}$ measurement, an unbinned likelihood fit to the $b\bar{b}$ invariant mass spectrum is performed in three p_T bins, $450 < p_T < 500$ GeV, $500 < p_T < 600$ GeV and $600 < p_T < 1000$ GeV. $\mu_{pre-tag}$ is obtained in both cases using the $Z \rightarrow l^+l^-$ channel since overwhelming backgrounds make a measurement in the $Z \rightarrow b\bar{b}$ channel unfeasible. The results are shown in Figure 4. The uncertainty in the $Z(\rightarrow b\bar{b})\gamma$ measurement is dominated by statistics, whereas for the $Z(\rightarrow b\bar{b}) + \text{jets}$ measurement, the leading source of uncertainty is from the fit model in the first two bins and from the modelling of the $Z + \text{jets}$ background in the third.

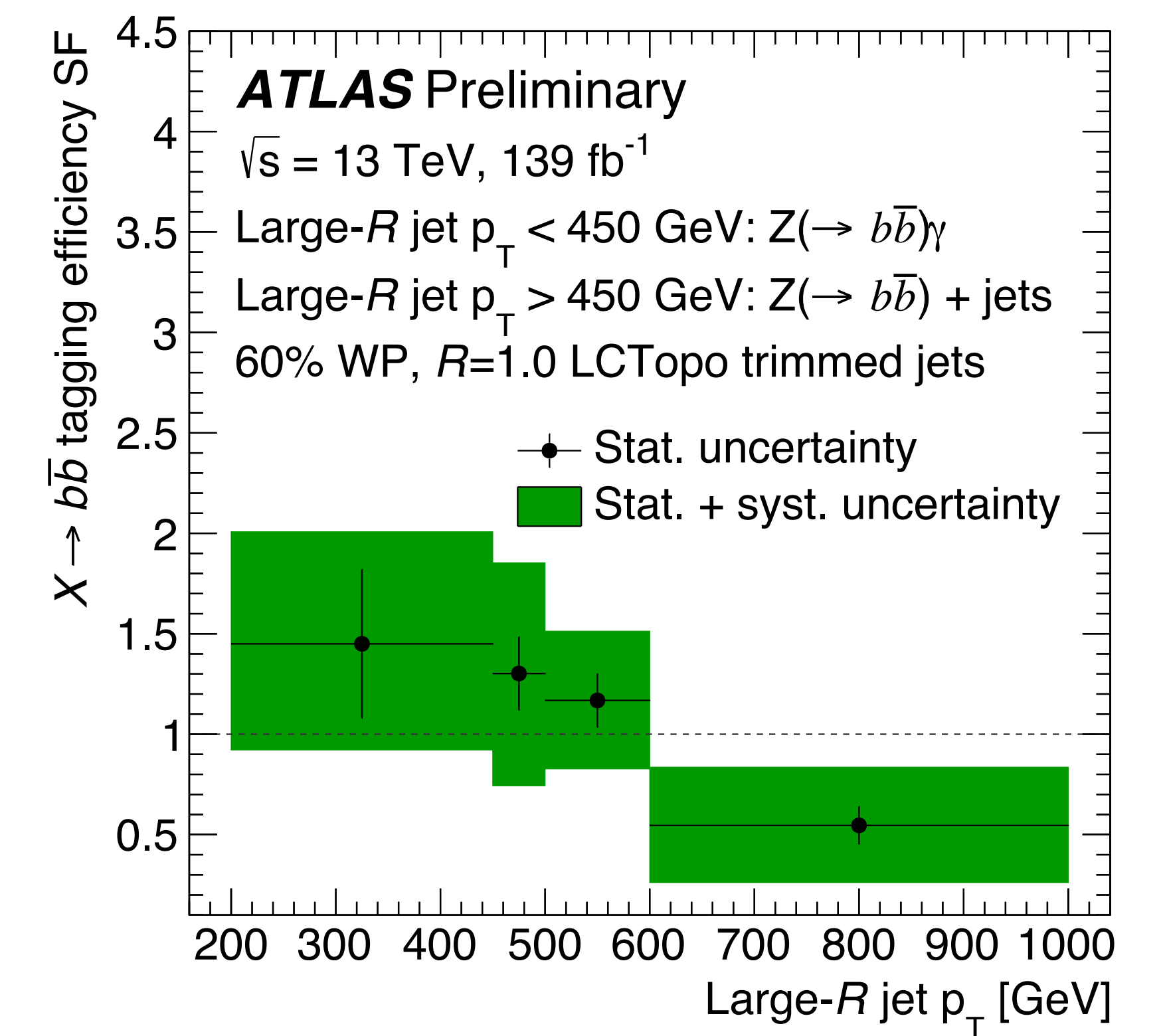


Figure 4: Signal efficiency scale factors for the $X \rightarrow b\bar{b}$ tagger at the 60% operating point [3].

Mis-tag efficiency calibration using $t\bar{t}$ decays

The mis-tag efficiency is defined as the probability to misidentify a top-quark jet as a signal event and is measured using single-lepton $t\bar{t}$ events in which one W boson decays leptonically and the other decays hadronically. Two signal regions are created, based on whether the leading large- R jet passes or fails the $X \rightarrow b\bar{b}$ tagger. The mis-tag efficiency scale factor is extracted in four bins of p_T , $300 < p_T < 400$ GeV, $400 < p_T < 500$ GeV, $500 < p_T < 600$ GeV and $600 < p_T < 1000$ GeV, using a binned likelihood fit simultaneously in both signal regions to the large- R jet mass spectrum. This measurement is limited by the systematic uncertainties, with the leading source of uncertainty coming from the $t\bar{t}$ modelling; however, a precision of smaller than 5-16% is still achieved. Figure 5 shows the results.

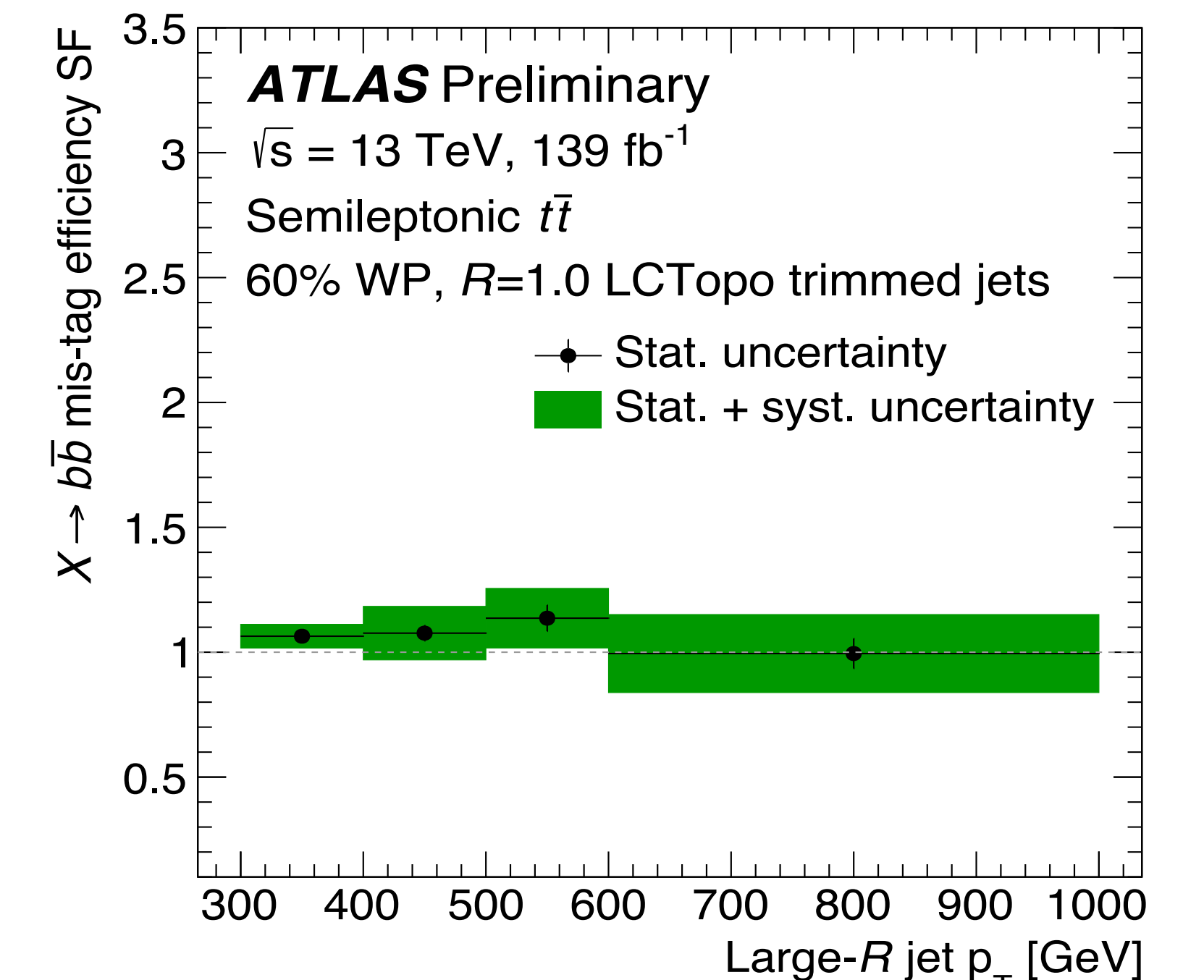


Figure 5: Mis-tag efficiency scale factors for the $X \rightarrow b\bar{b}$ tagger at the 60% operating point [3].

Modelling checks with $g \rightarrow b\bar{b}$ events

Multijet production is a significant background for many boosted Higgs analyses, particularly those with all-hadronic final states. Consequently, multijet events enriched in $g \rightarrow b\bar{b}$ events are used to verify the modelling of the large- R jet kinematics after the application of the tagger.

In order to use these events, a flavour composition correction is first performed using the mean of the signed d_0 significance, $\langle s_{d_0} \rangle$. The correction is determined as a function of p_T in three regions: $550 < p_T < 600$ GeV, $600 < p_T < 750$ GeV and $750 < p_T < 1000$ GeV. After the flavour fractions have been corrected, the modelling is then evaluated, as can be seen in Figure 6 for the large- R jet mass after tagging in the $550 < p_T < 600$ GeV range.

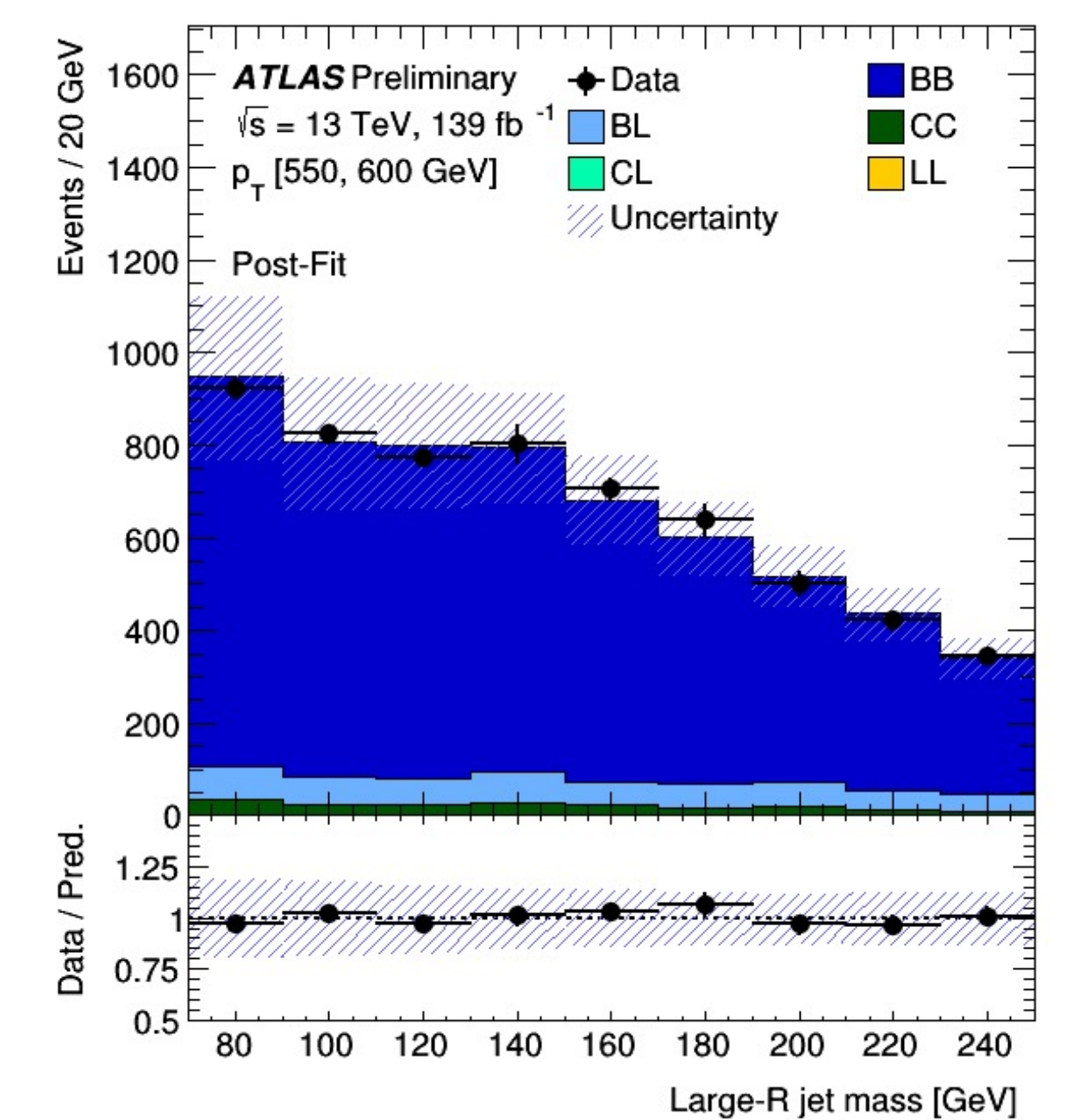


Figure 6: Large- R jet mass after tagging at the 60% operating point for $550 < p_T < 600$ GeV [3].

- [1] Moreno, E., Nguyen, T., Vlimant, J., Cerri, O., Newman, H., Perival, A., Spiropulu, M., Duarte, J. and Pierini, M., *Interaction networks for the identification of boosted $H \rightarrow b\bar{b}$ decays*, *Phys. Rev. D* **102** (2020) 1, arXiv: 1909.12285 [hep-ex]
- [2] ATLAS Collaboration, *Identification of Boosted Higgs Bosons Decaying Into $b\bar{b}$ With Neural Networks and Variable Radius Subjets in ATLAS*, ATL-PHYS-PUB-2020-019, 2020, URL: <https://cds.cern.ch/record/2724739>
- [3] ATLAS Collaboration, *Efficiency corrections for a tagger for boosted $H \rightarrow b\bar{b}$ decays in pp collisions at $\sqrt{s} = 13$ TeV with the ATLAS detector*, ATL-PHYS-PUB-2021-035, 2021, URL: <https://cds.cern.ch/record/2777811>